



HAL
open science

Past and present ITRF solutions from geophysical perspectives

Laurent Métivier, Zuheir Altamimi, Hélène Rouby

► **To cite this version:**

Laurent Métivier, Zuheir Altamimi, Hélène Rouby. Past and present ITRF solutions from geophysical perspectives. *Advances in Space Research*, 2020, 65, pp.2711-2722. 10.1016/j.asr.2020.03.031 . insu-03748806

HAL Id: insu-03748806

<https://insu.hal.science/insu-03748806>

Submitted on 12 May 2023

HAL is a multi-disciplinary open access archive for the deposit and dissemination of scientific research documents, whether they are published or not. The documents may come from teaching and research institutions in France or abroad, or from public or private research centers.

L'archive ouverte pluridisciplinaire **HAL**, est destinée au dépôt et à la diffusion de documents scientifiques de niveau recherche, publiés ou non, émanant des établissements d'enseignement et de recherche français ou étrangers, des laboratoires publics ou privés.



Distributed under a Creative Commons Attribution 4.0 International License



Past and present ITRF solutions from geophysical perspectives

Laurent Métivier^{*}, Zuheir Altamimi, Hélène Rouby

IPGP, IGN, Université Paris-Diderot, Sorbonne Paris-Cité, CNRS UMR7154, Bâtiment Lamarck, 35 rue Hélène Brion, 75013 Paris, France

Received 19 November 2019; received in revised form 19 March 2020; accepted 23 March 2020

Available online 6 April 2020

Abstract

Questions about the accuracy of the origin of the different versions of International Terrestrial Reference Frame (ITRF), have been regularly raised. In particular the origin drift between ITRF2000 and ITRF2005 (and subsequent ITRF solutions) is well-known to be problematic. Here, we look forward a sort of geophysical evaluation of ITRF solutions. We investigate GNSS vertical velocities provided by the last four ITRF solutions (ITRF2000 to ITRF2014; Altamimi et al., 2005, 2007, 2011, 2016) that we compare with different Global Isostatic Adjustment (GIA) model predictions. We find that each new ITRF solution appears to be more and more consistent with all GIA predictions, except ITRF2014 whose consistency with the GIA models depends on the date of observation. Indeed, GNSS observations and GIA predictions appear consistent at global scale at a level of ~ 4 mm/yr using ITRF2000 data, ~ 2.5 – 3 mm/yr using ITRF2005 data, and ~ 2 mm/yr using ITRF2008 data (global weighted root mean squares). For ITRF2014, the consistency between GNSS observations and GIA predictions is extremely high in 2000 (~ 1.5 mm/yr) but seems then to decrease with time (~ 2 mm/yr in 2013). This discrepancy is due to the recent ice melting effect that is not accounted for in GIA models, but clearly evidenced by ITRF2014 vertical velocities during the last years of observations, in particular in Greenland.

© 2020 COSPAR. Published by Elsevier Ltd. This is an open access article under the CC BY license (<http://creativecommons.org/licenses/by/4.0/>).

Keywords: ITRF; GNSS; Vertical velocities; Glacial Isostatic Adjustment; Current ice melting

1. Introduction

Studying and understanding Earth system global dynamics rely fundamentally on the definition and the realization of a global terrestrial reference system. Indeed, observing plate tectonic, co/postseismic deformations, global geophysical fluid dynamics, impacts of climate change and sea level rise, or determining satellite orbits, require estimating point positions and velocities at the Earth surface with a few millimetres or mm/yr accuracy. This can be achieved today using space geodesy provided that measurements are correctly referenced to a self-consistent and precise global geodetic reference frame. For this purpose, the International Terrestrial Reference Frame (ITRF), as a numerical realization of the International Terrestrial Ref-

erence System (ITRS), has been defined, realized and maintained under the framework of the International Earth Rotation and Reference Systems Service (IERS) for more than thirty years. Since the creation of IERS in 1988, thirteen ITRF versions were published, starting with the ITRF88 and ending with ITRF2014 that is currently used in operational geodesy and earth science applications. The space geodetic techniques that contribute to the ITRF construction are Very Long Baseline Interferometry (VLBI), Satellite Laser Ranging (SLR), Global Navigation Satellite Systems (GNSS) and Doppler Orbitography Radiopositioning Integrated by Satellite (DORIS). These techniques are organized as scientific services within the International Association of Geodesy (IAG) and known by the IERS as Technique Centers (TCs): the International VLBI Service (IVS), ([Schuh and Behrend, 2012](#)), the International Laser Ranging Service (ILRS), ([Pearlman et al., 2002](#)), the International GNSS Service, formerly the

^{*} Corresponding author.

E-mail address: laurent.metivier@ign.fr (L. Métivier).

International GPS Service (IGS), (Dow et al., 2009) and the International DORIS Service (IDS), (Moreaux et al., 2016).

Here we focus on some geophysical features of the latest four ITRF solutions: ITRF2000 (Altamimi et al., 2002), ITRF2005 (Altamimi et al., 2007), ITRF2008 (Altamimi et al., 2011) and ITRF2014 (Altamimi et al., 2016). As we will see below, all these solutions provide geodetic station velocities on different global networks, which all together can give a global overview of the decadal to secular time evolution of the solid Earth figure (Métivier et al., 2012). While the formal precision of the different ITRF solutions has improved over time, questions about the accuracy of the different solutions have been regularly raised. In particular an origin drift of ~ 1.8 mm/yr on the Z-component is present between ITRF2000 and ITRF2005 (and therefore subsequent ITRF solutions whose origins are closer to ITRF2005 origin). Such a changes in the velocity of the frame center has been shown to be problematic, notably for studies of plate motion and Glacial Isostatic Adjustment (GIA) (Argus 2007) and sea level rise estimations based on satellite altimetry (Morel and Willis, 2005; Beckley et al., 2007). A few studies have led to results that suggested that ITRF2000 was more accurate than ITRF2005, based on tectonic or local Glacial Isostatic Adjustment (GIA) estimations (Argus, 2007; Kogan and Steblov, 2008; Lidberg et al., 2009; Elliott et al., 2010). Today, even if many publications, in particular the publications of ITRF2008 and ITRF2014, have globally dispelled the concerns (e.g., Altamimi et al., 2011; Argus et al., 2014; Altamimi et al., 2016), some doubt on the accuracy of the ITRF origin with respect to ITRF2000 still remain sometimes (e.g. Tregoning et al., 2009; Mémin et al., 2011; Kierulf et al., 2014; Lambeck et al., 2017). ITRF is centered on the Center of Mass (CM) of the Earth as sensed by the Satellite Laser Ranging (SLR) technique only. Of course there is an uncertainty in the CM velocity estimation from SLR. Wu et al. (2011) and Argus (2012), using different approaches, concluded that CM velocity in ITRF2008 was determined at ± 1 mm/yr (2 sigma). For ITRF2014, using 5 years more data, Riddell et al. (2017) concluded that the CM velocity uncertainty was closer to ± 0.66 mm/yr (2 sigma). Another difficulty arises from the fact that the CM may have recently accelerated (Métivier et al., 2020). Evaluating the accuracy of an ITRF solution is complex and challenging, because of the extreme and unique precision of each ITRF solution. One way is to compare ITRF observations, in particular long-term stations velocities, with geophysical independent observations and models.

All ITRF stations, in particular GNSS stations, show long term, mostly linear, displacements. The station velocities are mainly dominated by their horizontal component with a magnitude of few cm/yr, which has been shown to be dictated by plate tectonics. As a consequence, plate tectonic motions have been re-estimated after each ITRF solution publications since ITRF2000, using ITRF GNSS

station horizontal velocity estimations (Altamimi et al., 2002, 2007, 2012, 2017). While those plate tectonic model are globally consistent with other tectonic models (e.g., Argus and Gordon, 1991; DeMets et al., 2010; Argus et al., 2011), small differences remain at the level of a few mm/yr locally (Altamimi et al., 2012). A few attempts to use tectonic motion have been made in the past to evaluate the accuracy of the different ITRF solutions (e.g. Argus, 2007; Kogan and Steblov, 2008; Argus et al., 2010). However it appears today that geodetic plate motion models are probably polluted by a GIA signal. Indeed, the GIA induces intraplate horizontal deformation far from past ice sheets that can be misinterpreted as tectonic motions (Argus and Peltier, 2010; Calais et al., 2017; Kierulf et al., 2014; Altamimi et al., 2017; Kreemer et al., 2018). Unfortunately the global ground horizontal motion induced by the GIA is poorly known and particularly difficult to estimate due to the potential impact of low viscosity layers in the upper part of the mantle. Therefore, today, most GIA models do not provide horizontal velocities, with the notable exception of ICE-5G and ICE-6G models (Peltier, 2004; Argus et al., 2014; Peltier et al., 2015). However these two models provide extremely different horizontal velocities over North America. These issues make horizontal velocities presently difficult to exploit for an ITRF geophysical evaluation.

On the other hand, station vertical velocities are clearly smaller than horizontal velocities, but, as we will see below, better adapted for an ITRF geophysical evaluation. Large GNSS station velocities can be seen over Canada and Fennoscandia, which are most probably due to GIA. Relatively large vertical velocities may also be observed in certain ITRF solutions for stations located in presently glaciated areas, in particular Greenland, Antarctica, Alaska, Iceland, Svalbard, etc. While GIA in Canada and Fennoscandia is the result of ice sheets retreat since the last glacial maximum (~ 20 – 30 kyr BP), the ground vertical velocities observed over current glaciated areas are most probably induced by Recent Ice Melting (RIM) (e.g., Cazenave and Lovel, 2010; Shepherd et al., 2012). Both phenomena induce deformation of the solid Earth (e.g., Peltier, 1974; Khan et al., 2010), sea level variations (e.g., Peltier, 1998; Lambeck and Chappell, 2001), gravity time variations (e.g. Tamisiea et al., 2007; Khan et al., 2010), geocenter motions (Greff-Lefitz, 2000; Argus, 2007; Greff-Lefitz et al., 2010; Métivier et al., 2010, 2011), and rotation variations (e.g., Mitrovica et al., 2005; Chambers et al., 2010). Finally other sources of long-term vertical motions may be locally possible, e.g. co/postseismic deformation, hydrology, tectonic deformation, anthropogenic effects, etc. Here we investigate GNSS vertical velocities from all the ITRF solutions since ITRF2000, which we compare to various GIA models. We aim to extract information on the accuracy of the different frames and identify the causes of their differences. Finally, we investigate if we can give insights on GIA processes from ITRF solutions.

The present manuscript is organized as follow. After reviewing the specifics of the different past and up-to-date ITRF solutions, we present different GIA models and their vertical ground motion predictions, which we interpolate over the different ITRF GNSS networks and confront with ITRF estimations. Finally we discuss our results and conclude.

2. ITRS realizations and their specificities

2.1. Past ITRF solutions

From ITRF88 up to ITRF2000, the input solutions used were provided by individual analysis centers of the four techniques and were in the form of station positions at a given epoch and constant velocities. The GNSS contribution to the ITRF started with ITRF91 (Altamimi et al., 1993), provided by Jet Propulsion Laboratory (JPL), exploiting the GIG'91 observation campaign (Blewitt and Lichten, 1992) comprising 21 GPS stations. DORIS data analysis has improved over time (Soudarin and Cazenave, 1995; Willis et al., 2005, 2010; Moreaux et al., 2016) and its contribution to the ITRF started with ITRF94 (Boucher et al., 1996) where three solutions were included, provided by Center for Space Research, University of Texas at Austin, Institut Géographique National (IGN), and Groupe de Recherche de Géodésie Spatiale (GRGS), France.

Unlike the earlier ITRF solutions, ITRF2000 combined unconstrained space geodesy solutions that are free from any tectonic plate motion model (Altamimi et al., 2002). In addition, the ITRF2000 velocity field was used to estimate rotation poles for six major tectonic plates.

Unlike the earlier ITRF solutions where global long-term solutions were combined, ITRF2005 used as input data time series (weekly from satellite techniques and 24-h session-wise from VLBI) of station positions and daily Earth Orientation Parameters (EOPs). ITRF2005 revealed a translation rate bias of 1.8 mm/yr in the Z-component of ITRF2000 that was later confirmed by the ITRF2008 and ITRF2014 results, indicating an imprecise ITRF2000 origin. Furthermore, using a velocity field of 152 sites with an error less than 1.5 mm/yr an absolute plate motion model consistent with the ITRF2005 frame was determined, involving the rotation poles of 15 tectonic plates.

The ITRF2008 elaboration was a continuation of the same combination strategy used in the ITRF2005 computation, which is, using time series of station positions and daily EOPs of the four space geodetic techniques: VLBI, SLR, GPS and DORIS, spanning 29, 26, 12.5 and 16 years of observations, respectively (Altamimi et al., 2011). Using a velocity field of 206 sites an absolute plate motion model consistent with ITRF2008 was estimated involving 14 major plates and has a precision of the order of 0.3 mm/yr WRMS (Altamimi et al., 2012).

2.2. ITRF2014

ITRF2014 was a milestone of the ITRS realizations, in that nonlinear station motions were modelled with an enhanced combination strategy, including seasonal (annual and semi-annual) signals of station positions, co-seismic jump detections (Métivier et al., 2014), and post seismic deformation (PSD) for sites that were subject to major earthquakes. The seasonal signals were modelled using cosine and sine functions, while the PSDs were described via four parametric models: (1) (Log)arithmic, (2) (Exp) onential, (3) Log + Exp, and (4) Exp + Exp (Altamimi et al., 2016).

We demonstrated that estimating the seasonal signals reduces the formal errors of the velocity components by about 10%, and therefore improved the ITRF2014 velocity determination, leading to a more robust reference frame.

The PSD parametric models were determined by fitting the IGS GNSS contributed daily time series for sites where the PSD was judged to be visually significant. We counted 117 sites that were subject to 59 major earthquakes with significant PSDs. The adjustment of the PSD parametric models was operated separately for the east, north and up components, taking into account a piecewise linear function, annual and semi-annual signals. The GNSS fitted parametric models were then applied to station position time series before their stacking, including nearby stations of the three other collocated techniques. We showed that at these PSD collocated sites, the GNSS fitted parametric models also fit perfectly the time series of the nearby stations of the other three techniques, indicating the high performance of these models.

Using ITRF2014 velocity field of 297 sites far from plate boundaries, Glacial Isostatic Adjustment areas and deforming zones, an absolute plate motion model for 11 plates, fully consistent with ITRF2014 was estimated, with an overall uncertainty at the level of 0.3 mm/yr (Altamimi et al., 2017).

2.3. Stability of the ITRF defining parameters

We recall that in order to define a secular/linear reference frame, such as the ITRF, 14 parameters must be explicitly specified: 3 for the origin, 1 for the scale, 3 for the orientation, all given at a chosen epoch, and 7 corresponding parameters describing the time evolution of the frame. The ITRF origin and its time evolution are chosen to follow, linearly, the long-term origin of the SLR frame, through the ILRS contributed solutions. The ITRF scale and its rate are currently defined by the arithmetic average of the SLR and VLBI intrinsic scales. The ITRF orientation and its time evolution are specified by a no net rotation condition between the successive ITRF solutions.

While the ITRF orientation is conventionally defined and of least consequence, the other ITRF defining physical parameters, namely the origin and the scale are of critical importance for Earth science applications, and in particu-

lar their time evolution. An ITRF origin or scale drift will automatically propagate into the station velocities and in particular the vertical velocities which are investigated in this paper in order to quantify their content of geophysical information.

Table 1 lists the origin and scale offsets and drifts of ITRF2000, ITRF2005 and ITRF2008 with respect to ITRF2014, as extracted from Altamimi et al. (2011, 2016). From that table we can observe small origin offsets for ITRF2005 and ITRF2008, at the level of 3 mm in average. The large scale offset of 0.92 ppb for ITRF2005 is partly due to the fact that the scale of ITRF2005 was defined with respect to VLBI submitted solutions only, where the pole tide effect was not accounted for. The neglect of the pole tide effect has an estimated impact on the scale of the order of 0.5 ppb.

More importantly, the origin and scale drifts listed in Table 1 can be used to evaluate the stability of the ITRF origin and scale over time. From that table we can see that the origin and scale drifts, starting with ITRF2005, are stabilizing at the level of 0.3 mm/yr in average. The larger ITRF2000 origin drift with respect to ITRF2014 of 1.9 mm/yr in the Z-component is again an indication of its imprecise origin determination. This observation indicates that the geophysical results that can be extracted from ITRF2005 onward can be interpreted with confidence, and in particular the results from ITRF2014 which is demonstrated to be superior to the past two versions as the non-linear station motions were rigorously modelled.

3. ITRF GNSS vertical velocities: geophysical information

3.1. GIA modelling

We investigate different GIA models in the framework of this ITRF geophysical analysis: two versions of the ICE5G-VM2 model, the original one from Peltier (2004) and a derivative one from Paulson et al. (2007), the ICE6G-VM5a model from Peltier et al. (2015), and the Australian National University (ANU) ice model associated with five different viscosity profiles (Lambeck et al., 2010; Lambeck et al., 2014; Lambeck et al., 2017). Originally, the ANU GIA model made use of various viscosity profiles, one for each specific GIA region. Because we need global GIA deformation, and because the selection of a viscosity profile is still a subject of debate (e.g., Lambeck et al., 2014; Métivier et al., 2016), we calculated the global Earth response to the ANU ice history using five different

viscosity profiles, independently of the region concerned (models denoted hereafter ANU-V1 to ANU-V5). These profiles, in practice, reflect the mantle behavior under different types of crust and regions (continental, oceanic, margins, cratons...) (see Table 2 and Lambeck et al., 2014, 2017). By doing so, we expect to get a spectrum of realistic possible responses of the Earth to the ANU ice history. Finally, in order to more closely follow the specifics of ANU GIA model, we constructed a model which combines the different ANU solutions, i.e., using ANU-V1 for the ground deformation over North America, ANU-V2 over Europe and ANU-V4 for the rest of the world. We denote this last model ANU-COMB. We did not use ANU-V3 and ANU-V5 in our combination because these profiles are possible profiles for far-field regions (with respect to past ice sheet locations), typically under oceanic areas, whereas GPS stations are essentially located on continental areas. ANU-V4 is a mean viscosity profile for “middle-field” regions, typically under margin areas (Lambeck et al., 2014, 2017; Simms et al., 2016). Of course, all our GIA calculations include the classical resolution of the sea-level equation (e.g., Peltier, 1998; Lambeck and Chappell, 2001), using a code developed by Caron et al. (2017). Fig. 1 presents different examples of GIA vertical motion predictions. One can see that the largest vertical velocities (larger than 2 mm/yr) are, as expected, over Canada, Fennoscandia, and Antarctica.

3.2. Vertical velocities

Fig. 2 presents the GNSS vertical velocities associated with the ITRF2000, ITRF2005 and ITRF2008 solutions. In this figure, stations that show evidence of postseismic or anthropogenic deformation have been excluded. As expected, one can see large GNSS station velocities, up to 15–20 mm/yr, over Canada and Fennoscandia. Fig. 3 shows the GNSS vertical velocities of the ITRF2014. In the ITRF2014 solution we had to introduce velocity discontinuities in a few GNSS time series in order to fully account for the long-term non-linearity behavior of a few specific stations. If we exclude station subjected to post-seismic deformations, most of these stations are located in Greenland, a few in Antarctica, Alaska, and Iceland (see e.g., Métivier et al., 2020, for ITRF2014 GNSS time series in Greenland). As a consequence, in the ITRF2014 solution, we are able to track down vertical velocity changes in these regions. For this reason Fig. 3 presents GNSS vertical velocities at three different dates. One can

Table 1
Origin and scale offsets and drifts of past ITRF solutions with respect to ITRF2014.

ITRF	Origin offset			Origin drift			Scale offset D ppb	Scale drift \dot{D} ppb/yr
	T_x mm	T_y mm	T_z mm	\dot{T}_x mm/yr	\dot{T}_y mm/yr	\dot{T}_z mm/yr		
2000	0.7	1.2	−26.1	0.1	0.1	1.9	2.12	0.11
2005	2.6	1.0	−2.3	0.3	0.0	−0.1	0.92	0.03
2008	1.6	1.9	2.4	0.0	0.0	−0.1	−0.02	0.03

Table 2

The different viscosity profiles used for calculating the global GIA response to ANU ice history model.

	V1	V2	V3	V4	V5
Lithosphere thickness (km)	100	90	60	50	80
Upper mantle viscosity (Pa s)	5.0×10^{20}	3.0×10^{20}	1.5×10^{20}	1.5×10^{20}	2.0×10^{20}
Lower mantle viscosity (Pa s)	1.5×10^{22}	1.0×10^{22}	2.0×10^{21}	7.0×10^{22}	1.0×10^{22}

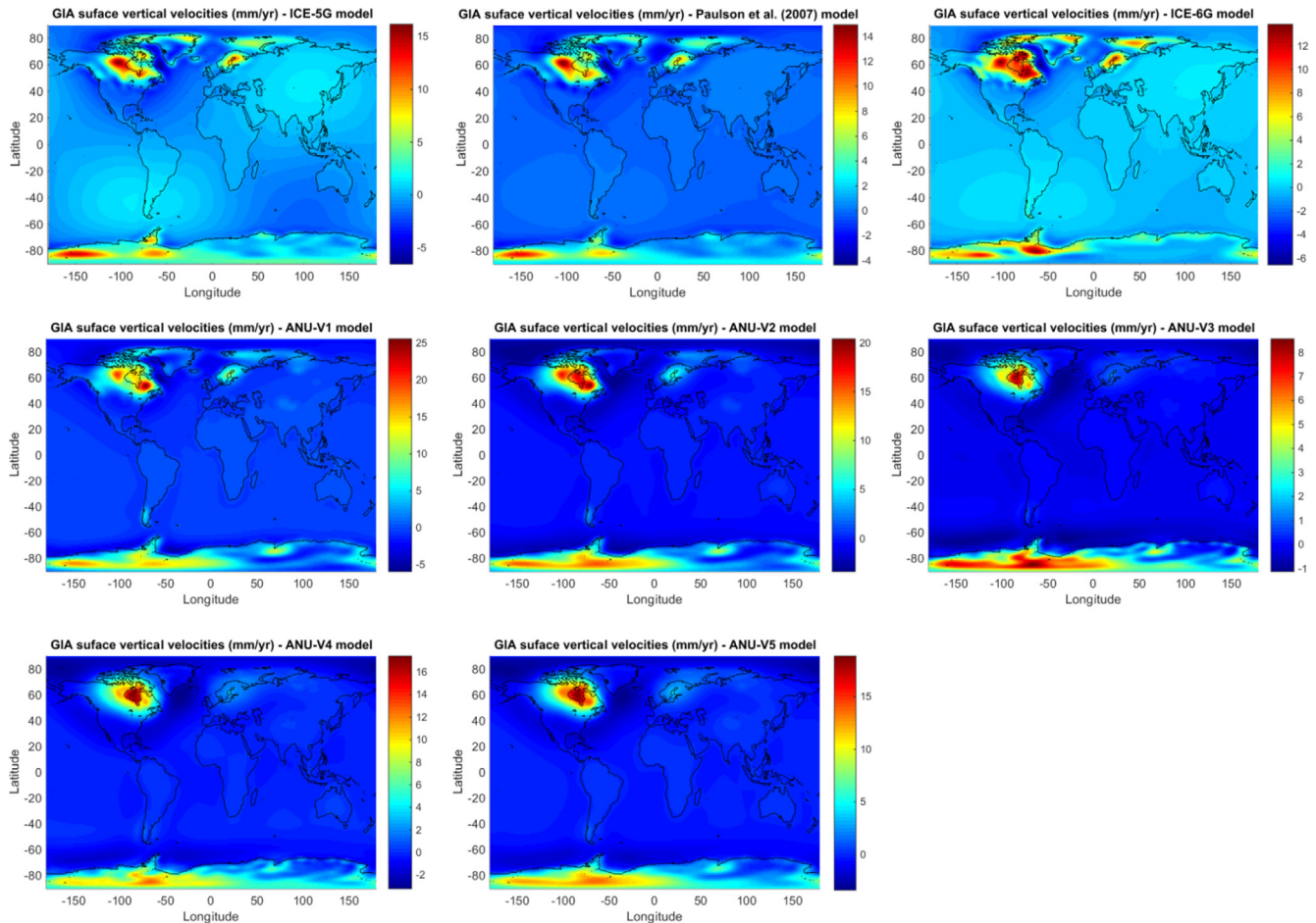


Fig. 1. Different model predictions of the solid Earth vertical motion induced today by GIA processes.

also see that the GNSS network has evolved over time: many new stations have been installed in Greenland during the late years of the GNSS data analysis time period. In this last figure, stations that present evidence of postseismic or anthropogenic deformations have been also excluded.

We evaluated the different GIA solutions presented in Section 3.1 on each site in any of the ITRF GNSS networks (Figs. 2 and 3). Fig. 4 presents the vertical velocity differences between the main GIA models expressed over ITRF2014 network, with respect to ICE-6G model. One can see that GIA models give predictions relatively different in particular over Canada region. While ICE-5G gives larger velocity than ICE-6G over the western part of Canada, ANU-COMB gives larger velocity than ICE-6G mostly over the eastern part of Canada. On the other hand, ICE-6G vertical velocity predictions are particularly larger

than ANU-COMB velocities over Greenland and Fennoscandia.

We then compared the different GIA predictions with the ITRF GNSS vertical velocities estimations of the different networks. Fig. 5 presents the results of this comparison. Weighted Root Mean Squares (RMS) of the difference between estimations and predictions are presented for all ITRF solutions and all GIA models. In these comparisons we only kept stations whose vertical velocities have been estimated with precision better than 1 cm/yr. This represents 87% of GNSS stations in ITRF2000 solution, 98% of the stations in ITRF2005 solution, 99% of stations in ITRF2008 and ITRF2014 solutions. The results presented in Fig. 4 are analysed and discussed in the next section. Note that the number of stations that have been used for the RMS calculations varies. The number of station

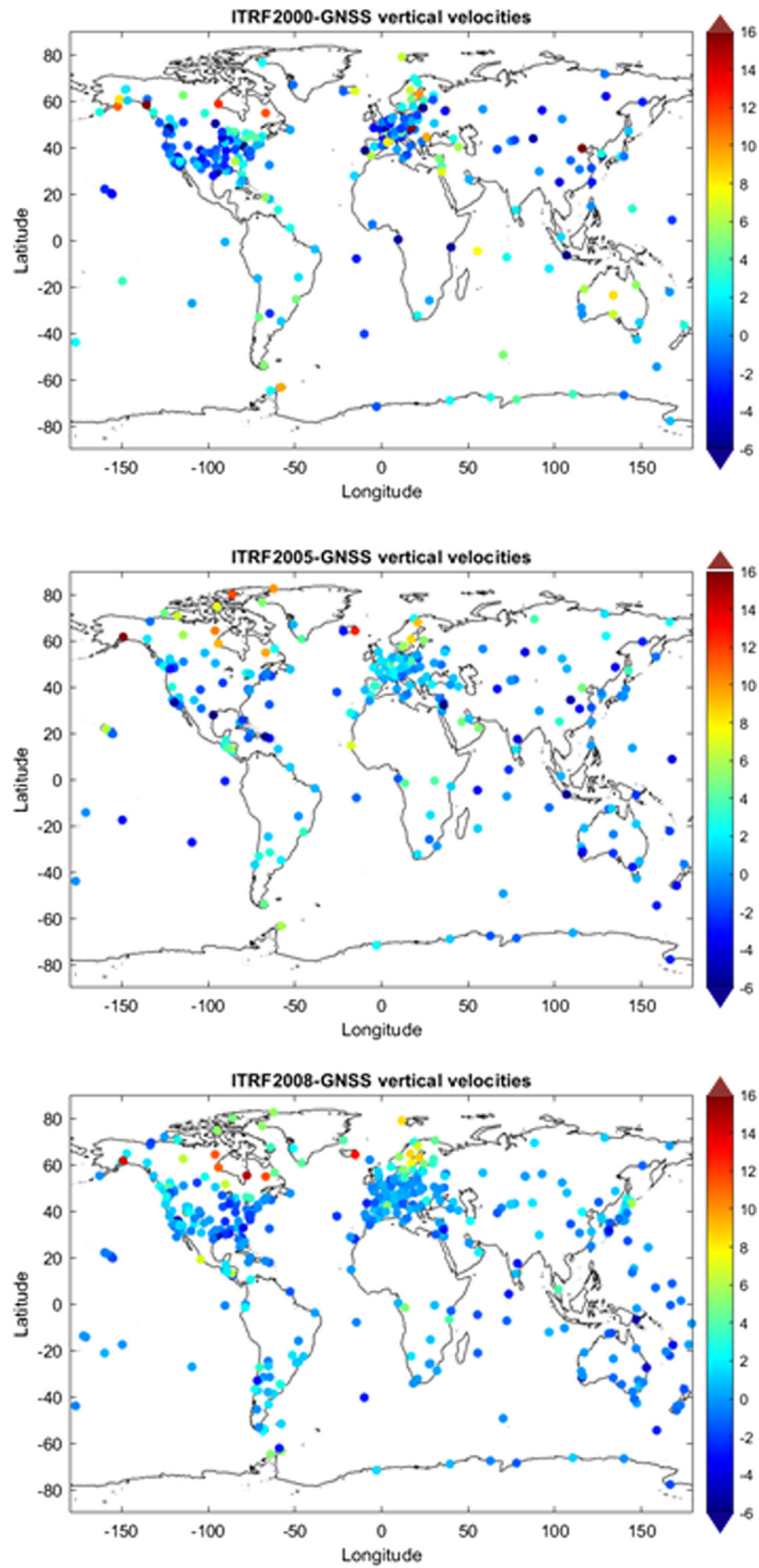


Fig. 2. From top to bottom: ITRF2000, ITRF2005 and ITRF2008 GNSS station vertical velocities. Stations whose position time series present evidence of postseismic or anthropogenic deformations are not shown here.

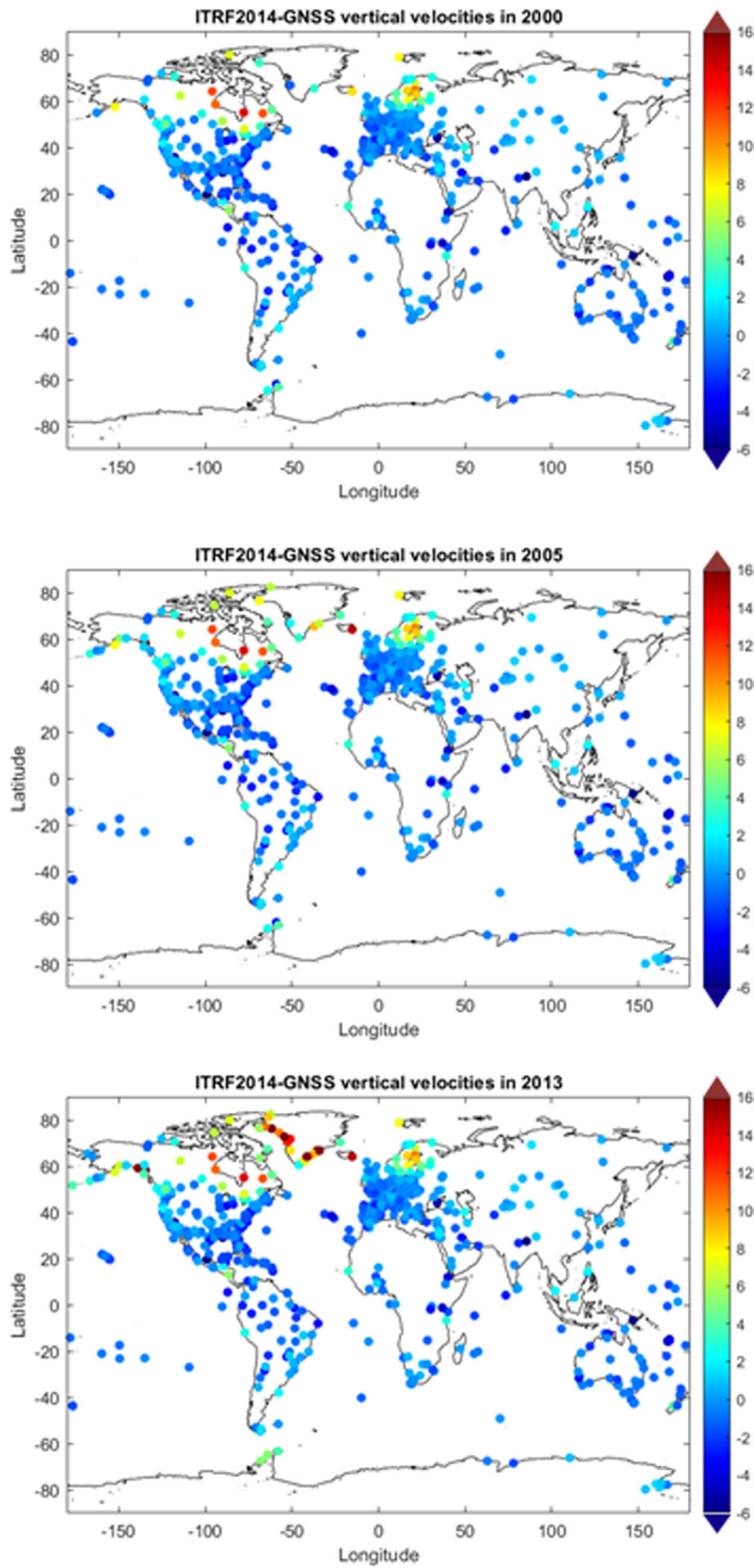


Fig. 3. ITRF2014 GNSS station vertical velocities at dates 2000 (top), 2005 (middle) and 2013 (bottom). Stations whose position time series present evidence of postseismic or anthropogenic deformations are not shown here.

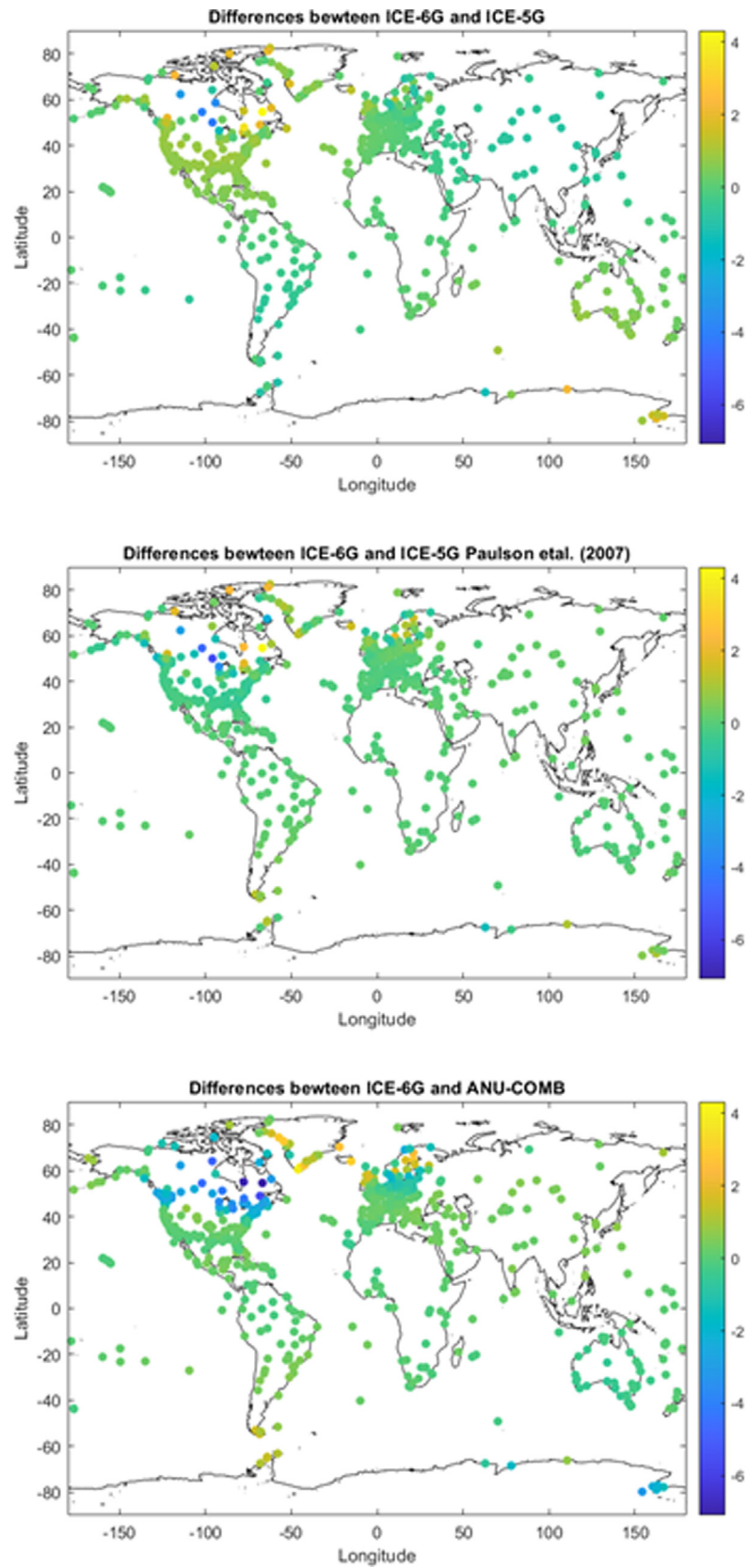


Fig. 4. Vertical velocity differences between ICE-6G GIA model and three other GIA models expressed over ITRF2014 GNSS station network at date 2013.

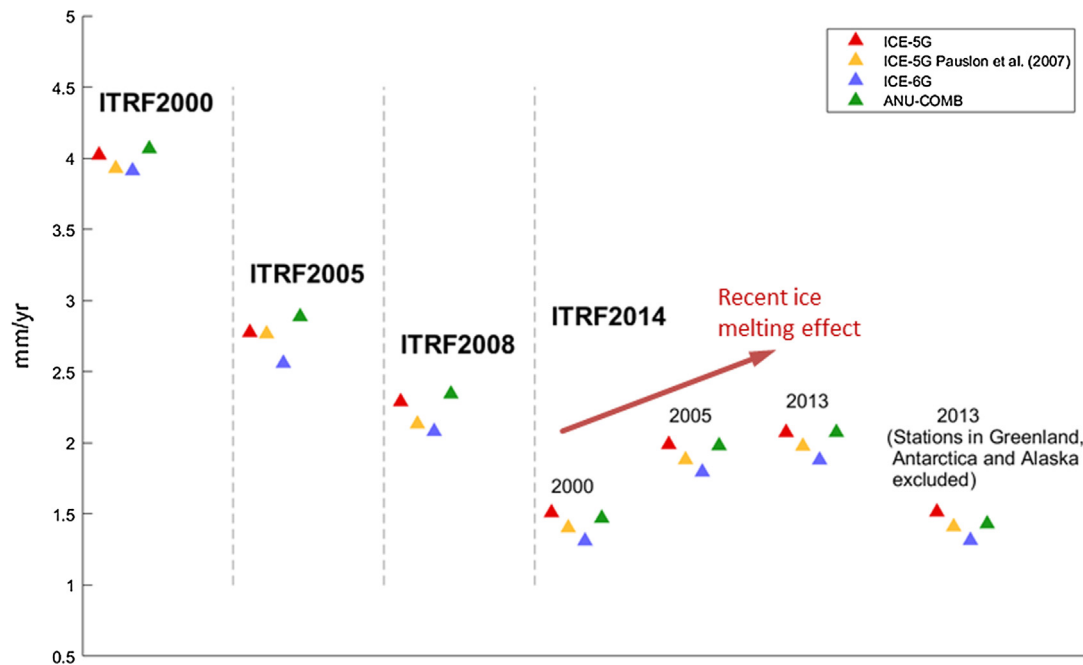


Fig. 5. Weighted Root Mean Squares (RMS) of the difference between ITRF vertical velocity estimations and four GIA vertical velocity predictions, depending on ITRF solutions and GIA models. For the ITRF2014 solution, the RMS have been estimated at different dates (dates 2000, 2005 and 2013) in order to account for the vertical velocity changes of a few ITRF2014 GNSS stations.

increase, in particular in Greenland, could therefore bias the RMS results at different dates. In order to be sure that biases are small we conducted different tests. In this regard, the weighting of the RMS calculation is important because the vertical velocity uncertainties are generally smaller when the time of observations is larger. Therefore the increase of stations is partly compensated by the weighting. We also made tests using only common stations at the different dates and we found that it affects RMS value less than $\sim 10\%$. Considering the values that are presented in Fig. 5, we concluded that the impact of the number of station is therefore not significant.

4. Discussion and conclusions

In Fig. 5, one can see that all the investigated ITRF solutions are globally consistent with the four main GIA models that we used: ICE-5G, ICE-5G from Paulson et al. (2007), ICE-6G and ANU-COMB. The level of agreement ranges between ~ 1 and ~ 4.5 mm/yr (RMS). For a given ITRF solution, the difference in RMS misfit between the GIA models appear quite small, less than ~ 0.5 mm/yr. However the RMS clearly diminishes with the ITRF solutions, independent of the GIA model considered, going from ~ 4 mm/yr for ITRF2000 to ~ 3 mm/yr for ITRF2005, ~ 2 mm/yr for ITRF2008, and ~ 1.5 mm/yr for ITRF2014 at date 2000. This means that, since ITRF2000, each new ITRF solution has shown a vertical velocity configuration more and more consistent with GIA predictions in general. We believe that it is an important indication of the global improvement of ITRF solutions over time. Yet, ITRF con-

sistency with GIA processes has often been the argument put forward by different authors to qualify ITRF2000 as more accurate than subsequent ITRF solutions. A reason that may explain these previous studies is that they essentially focused on regional observations, mostly in Fennoscandia, with GIA models that are outdated today (e.g. Lidberg et al., 2009). Here we see that the GNSS vertical velocities of the ITRF2000 solution are clearly less consistent with the most up-to-date GIA models at global scale. The diminution of RMS is above all an indication of the worldwide improvement of vertical velocity estimations in the most recent ITRF solution, thanks to GNSS reanalysis campaigns (e.g., Rebischung et al., 2016). In Fig. 2, one can see that the ITRF2000 solution shows many station with large vertical velocities far from GIA regions, e.g. in Australia or in South Europe. ITRF2005 and ITRF2008 solutions show a vertical velocity configuration clearly more regionally homogeneous, with vertical velocities, for instance, nearly zero over Australia and South Europe. This homogeneity in the vertical velocity field is also visible in ITRF2014 solution at all dates.

The consistency of the ITRF2014 solution with the GIA models is evaluated at multiple epochs. As shown in Fig. 4, the consistency between ITRF2004-GNSS vertical velocities and GIA vertical velocities is extremely good in 2000, with an RMS around 1.5 mm/yr. But the RMS increases with time, up to 2–2.5 mm/yr in 2013. This is actually the sign that a geophysical process, not explained by the GIA models, is in progress. ITRF2014 vertical velocities at epoch 2000 are very similar to the ITRF2008 vertical velocities, which reflect mostly GIA predictions (see Figs. 2 and

3). But, in Fig. 3, we see that the ITRF2014 vertical velocities have then evolved in 2005 and in 2013. In 2013 the largest vertical velocities are no longer over Canada but over Greenland. This is undoubtedly due to Recent Ice Melting (RIM). While signs of RIM were already visible in the ITRF2008 solution (e.g., in Alaska, Iceland and Greenland), the impact of RIM has clearly increased since then. It has become the major source of vertical velocities during the later years of the ITRF2014 solution. This explains the increase in RMS between ITRF2014 and GIA predictions and confirms all the studies that mentioned RIM in Greenland and possible acceleration of the process (e.g., Khan et al., 2010; Rignot et al., 2011; Shepherd et al., 2012; Velicogna et al., 2014).

Given the RMS, ICE-6G model seems a better than other GIA models with respect to all ITRF GNSS solutions. But we must recall that ICE-5G and ICE-6G model have been constrained with GNSS observations, while ANU models were not (Peltier et al., 2015; Lambeck et al., 2017). This emphasizes the interest of using precise estimation of GNSS velocities in the determination of GIA processes. Fig. 6 presents the RMS for ANU-V1 to ANU-V5 models with respect to ITRF2014 at date 2000. We observe that combining different ANU solutions, in accordance with ANU specifications (Lambeck et al., 2014, 2017; Simms et al., 2016), clearly improves the fit. The gain in RMS is not clear compared with ANU-V1. But it should be noted that a GIA solution that combines different GIA global solutions, would not produce coherent sea level fingerprints and rotational feedback (e.g., Lambeck and Chappell, 2001; Mitrovica et al., 2005). Impacts of sea level variations and of the rotational feedback are relatively small on the present day vertical motion, but at global scale their correctness should slightly improve the fit with ITRF vertical velocities. For a complete calculation of the ANU model, one would need to use a code able to take into account lateral variations of viscosity. Realizing such a calculation at global scale is

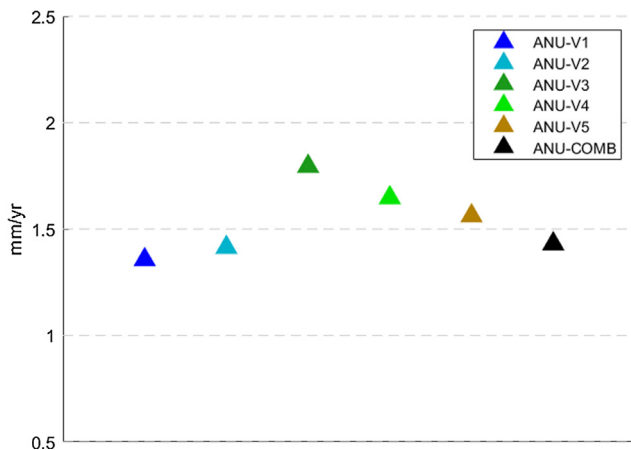


Fig. 6. RMS difference between ITRF2014 vertical velocity estimations (at date 2013) and GIA vertical velocity predictions from the different ANU models.

challenging due to theoretical and numerical reasons (see, e.g.; Wu et al., 2005; Latychev et al., 2005a; Métivier et al., 2006), and only rare GIA codes, today, are able to partially realize it (Latychev et al., 2005b; A et al., 2013; van der Wal et al., 2015). But, while such type of GIA calculations will probably be mandatory in the future for GIA investigations, the effect on our comparison should be small.

Here we only investigated station vertical velocities. It would be very interesting to include horizontal velocities in the analysis. However, as we mentioned before, the horizontal velocities are mostly dictated by plate tectonics and, unfortunately, the difference between ITRF GNSS observations and plate tectonic models is probably polluted by a GIA signal that is poorly known. It would be interesting in the future to develop joint inversions of plate tectonics and GIA models from GNSS station horizontal velocities and see their consistency with our results with vertical velocities (e.g., Ding et al., 2019).

Acknowledgements

We thank Donald Argus and two anonymous reviewers for their constructive and helpful reviews of our initial manuscript. We thank Kurt Lambeck and Anthony Purcell for their help and support in the exploitation of ANU model. Finally, we thank the Centre National d'Etudes Spatiales (CNES) for their financial support through the TOSCA committee. This is IPGP contribution number 4132.

References

- A, G., Wahr, J., Zhong, S., 2013. Computations of the viscoelastic response of a 3-D compressible Earth to surface loading: an application to Glacial Isostatic Adjustment in Antarctica and Canada. *Geophys. J. Int.* 192, 557–572. <https://doi.org/10.1093/gji/ggs030>.
- Altamimi, Z., Boucher, C., Duhem, L., 1993. The worldwide centimetric terrestrial reference frame and its associated velocity field. *Adv. Space Res.* 13 (11), 151–160.
- Altamimi, Z., Sillard, P., Boucher, C., 2002. ITRF2000: a new release of the International Terrestrial Reference Frame for earth science applications. *J. Geophys. Res.* 107 (B10), 2214. <https://doi.org/10.1029/2001JB000561>.
- Altamimi, Z., Collilieux, X., Legrand, J., Garayt, B., Boucher, C., 2007. ITRF2005: a new release of the international terrestrial reference frame based on time series of station positions and earth orientation parameters. *J. Geophys. Res.* 112, B09401. <https://doi.org/10.1029/2007JB004949>.
- Altamimi, Z., Collilieux, X., Métivier, L., 2011. ITRF2008: an improved solution of the International Terrestrial Reference Frame. *J. Geod.* 85, 457–473. <https://doi.org/10.1007/s00190-011-0444-4>.
- Altamimi, Z., Métivier, L., Collilieux, X., 2012. ITRF2008 plate motion model. *J. Geophys. Res.* 117, B07402. <https://doi.org/10.1029/2011JB008930>.
- Altamimi, Z., Rebeschung, P., Métivier, L., Collilieux, X., 2016. ITRF2014: a new release of the International Terrestrial Reference Frame modeling nonlinear station motions. *J. Geophys. Res.* 121, 6109–6131. <https://doi.org/10.1002/2016JB013098>.
- Altamimi, Z., Métivier, L., Rebeschung, P., Rouby, H., Collilieux, X., 2017. ITRF2014 plate motion model. *Geophys. J. Int.* 209 (3), 1906–1912. <https://doi.org/10.1093/gji/ggx136>.

- Argus, D.F., 2007. Defining the translational velocity of the reference frame of Earth. *Geophys. J. Int.* 169, 830–838. <https://doi.org/10.1111/j.1365-246X.2007.03344.x>.
- Argus, D.F., 2012. Uncertainty in the velocity between the mass center and surface of Earth. *J. Geophys. Res.* 117, B10405. <https://doi.org/10.1029/2012JB009196>.
- Argus, D.F., Gordon, R.G., 1991. No-net-rotation model of current plate velocities incorporating plate motion model NUVEL-1. *Geophys. Res. Lett.* 18 (11), 2039–2042. <https://doi.org/10.1029/91GL01532>.
- Argus, D.F., Gordon, R.G., Heflin, M.B., Ma, C., Eanes, R.J., Willis, P., Peltier, W.R., Owen, S.E., 2010. The angular velocities of the plates and the velocity of Earth's centre from space geodesy. *Geophys. J. Int.* 180 (3), 913–960. <https://doi.org/10.1111/j.1365-246X.2009.04463.x>.
- Argus, D.F., Gordon, R.G., DeMets, C., 2011. Geologically current motion of 56 plates relative to the no-net-rotation reference frame. *Geochem. Geophys. Geosyst.* 12 (11), Q11001. <https://doi.org/10.1029/2011GC003751>.
- Argus, D.F., Peltier, W.R., 2010. Constraining models of postglacial rebound using space geodesy: a detailed assessment of model ICE-5G (VM2) and its relatives. *Geophys. J. Int.* 181 (2), 697–723. <https://doi.org/10.1111/j.1365-246X.2010.04562.x>.
- Argus, D.F., Peltier, W.R., Drummond, R., Moore, A.W., 2014. The Antarctica component of postglacial rebound model ICE-6G_C (VM5a) based on GPS positioning, exposure age dating of ice thicknesses, and relative sea level histories. *Geophys. J. Int.* 198 (1), 537–563. <https://doi.org/10.1093/gji/ggu140>.
- Beckley, B.D., Lemoine, F.G., Luthcke, S.B., Ray, R.D., Zelensky, N.P., 2007. A reassessment of global and regional mean sea level trends from TOPEX and Jason-1 altimetry based on revised reference frame and orbits. *Geophys. Res. Lett.* 34, L14608. <https://doi.org/10.1029/2007GL030002>.
- Blewitt, G., Lichten, S.M., 1992. Carrier phase ambiguity resolution up to 12000 km: Results from the GIG'91 experiment. In: *Proc. of the Sixth Int. Symp. on Satellite Positioning*, Columbus, Ohio State University, USA.
- Boucher, C., Altamimi, Z., Feissel, M., Sillard, P., 1996. Results and Analysis of the ITRF94. IERS Technical Note 20, Central Bureau of IERS - Observatoire de Paris, p. 194.
- Calais, E., Fleitout, L., Lambeck, K., 2017. Eurasia-North America plate motion and Glacial Isostatic Adjustment. In: *AGU Fall Meeting Abstracts*, American Geophysical Union, Fall Meeting 2017, Abstract #G51C-02.
- Caron, L., Métivier, L., Greff-Lefftz, M., Fleitout, L., Rouby, H., 2017. Inverting Glacial Isostatic Adjustment signal using Bayesian framework and two linearly relaxing rheologies. *Geophys. J. Int.* 209 (2), 1126–1147. <https://doi.org/10.1093/gji/ggx083>.
- Cazenave, A., Lovel, W., 2010. Contemporary sea level rise. *Annu. Rev. Mar. Sci.* 2010 (2), 145–173. <https://doi.org/10.1146/annurev-marine-120308-081105>.
- Chambers, D.P., Wahr, J., Tamisiea, M.E., Nerem, R.S., 2010. Ocean mass from GRACE and glacial isostatic adjustment. *J. Geophys. Res.* 115, B11415. <https://doi.org/10.1029/2010JB007530>.
- DeMets, C., Gordon, R.G., Argus, D.F., 2010. Geologically current plate motions. *Geophys. J. Int.* 181 (1), 1–80. <https://doi.org/10.1111/j.1365-246X.2009.04491.x>.
- Ding, K., Freymueller, J.T., He, P., Wang, Q., Xu, C., 2019. Glacial isostatic adjustment, intraplate strain, and relative sea level changes in the eastern United States. *J. Geophys. Res.* 124, 6056–6071. <https://doi.org/10.1029/2018JB017060>.
- Dow, J., Neilan, R.E., Rizos, C., 2009. The international GNSS service in a changing landscape of global navigation satellite systems. *J. Geod.* 83 (3–4), 191–198. <https://doi.org/10.1007/s00190-008-0300-3>.
- Elliott, J.L., Larsen, C.F., Freymueller, J.T., Motyka, R.J., 2010. Tectonic block motion and glacial isostatic adjustment in southeast Alaska and adjacent Canada constrained by GPS measurements. *J. Geophys. Res.* 115, B09407. <https://doi.org/10.1029/2009JB007139>.
- Greff-Lefftz, M., 2000. Secular variation of the geocenter. *J. Geophys. Res.* 105 (B11), 25685–25692. <https://doi.org/10.1029/2000JB900224>.
- Greff-Lefftz, M., Métivier, L., Besse, J., 2010. Dynamic Mantle Density Heterogeneities and global geodetic observables. *Geophys. J. Int.* 180, 1080–1094. <https://doi.org/10.1111/j.1365-246X.2009.04490.x>.
- Khan, S.A., Wahr, J., Bevis, M., Velicogna, I., Kendrick, E., 2010. Spread of ice mass loss into northwest Greenland observed by GRACE and GPS. *Geophys. Res. Lett.* 37, L06501. <https://doi.org/10.1029/2010GL042460>.
- Kierulf, H.P., Steffen, H., James, M., Simpson, R., Lidberg, M., Wu, P., Wang, H., 2014. A GPS velocity field for Fennoscandia and a consistent comparison to glacial isostatic adjustment models. *J. Geophys. Res.* 119, 6613–6629. <https://doi.org/10.1002/2013JB010889>.
- Kogan, M.G., Steblov, G.M., 2008. Current global plate kinematics from GPS (1995–2007) with the plate-consistent reference frame. *J. Geophys. Res.* 113, B04416. <https://doi.org/10.1029/2007JB005353>.
- Kreemer, C., Hammond, W.C., Blewitt, G., 2018. A robust estimation of the 3-D intraplate deformation of the North American plate from GPS. *J. Geophys. Res.* 123, 4388–4412. <https://doi.org/10.1029/2017JB015257>.
- Lambeck, K., Chappell, J., 2001. Sea level change through the last glacial cycle. *Science* 292, 679–686.
- Lambeck, K., Purcell, A., Zhao, S., 2017. The North American Late Wisconsin ice sheet and mantle viscosity from glacial rebound analyses. *Quaternary Sc. Rev.* 158, 172–210. <https://doi.org/10.1016/j.quascirev.2016.11.033>.
- Lambeck, K., Purcell, A., Zhao, J., Svensson, N.-O., 2010. The Scandinavian ice sheet: from MIS 4 to the end of the last glacial maximum. *Boreas* 39, 410–435. <https://doi.org/10.1111/j.1502-3885.2010.00140.x>.
- Lambeck, K., Rouby, H., Purcell, A., Sun, Y., Sambridge, M., 2014. Sea level and global ice volumes from the Last Glacial Maximum to the Holocene. *Proc. Natl. Acad. Sci. USA* 111, 15296–15303. <https://doi.org/10.1073/pnas.1411762111>.
- Latychev, K., Mitrovica, J.X., Tromp, J., Tamisiea, M.E., Komatsich, D., Christara, C.C., 2005a. Glacial isostatic adjustment on 3-D Earth models: a finite-volume formulation. *Geophys. J. Int.* 161 (2), 421–444. <https://doi.org/10.1111/j.1365-246X.2005.02536.x>.
- Latychev, K., Mitrovica, J.X., Tamisiea, M.E., Tromp, J., Moucha, R., 2005b. Influence of lithospheric thickness variations on 3-D crustal velocities due to glacial isostatic adjustment. *Geophys. Res. Lett.* 32 (1), L01304. <https://doi.org/10.1029/2004GL021454>.
- Lidberg, M., Johansson, J.M., Scherneck, H.-G., Milne, G.A., Davis, J.L., 2009. New results based on reprocessing of 13 years continuous GPS observations of the Fennoscandia GIA process from BIFROST. In: *Observing our Changing Earth*. Springer, Berlin, Heidelberg, pp. 557–568.
- Mémin, A., Rogister, Y., Hinderer, J., Omang, O.C., Luck, B., 2011. Secular gravity variation at Svalbard (Norway) from ground observations and GRACE satellite data. *Geophys. J. Int.* 184 (3), 1119–1130. <https://doi.org/10.1111/j.1365-246X.2010.04922.x>.
- Métivier, L., Collilieux, X., Altamimi, Z., 2012. ITRF2008 contribution to glacial isostatic adjustment and recent ice melting assessment. *Geophys. Res. Lett.* 39, L01309. <https://doi.org/10.1029/2011GL049942>.
- Métivier, L., Collilieux, X., Lercier, D., Altamimi, Z., Beauducel, F., 2014. Global coseismic deformations, GNSS time series analysis, and earthquake scaling laws. *J. Geophys. Res.* 119, 9095–9109. <https://doi.org/10.1002/2014JB011280>.
- Métivier, L., Caron, L., Greff-Lefftz, M., Pajot-Métivier, G., Fleitout, L., Rouby, H., 2016. Evidence for postglacial signatures in gravity gradients: a clue in lower mantle viscosity. *Earth Planet. Sc. Lett.* 452, 146–156. <https://doi.org/10.1016/j.epsl.2016.07.034>.
- Métivier, L., Greff-Lefftz, M., Altamimi, Z., 2010. On secular geocenter motion: the impact of climate changes. *Earth Planet. Sc. Lett.* 296, 360–366. <https://doi.org/10.1016/j.epsl.2010.05.021>.
- Métivier, L., Greff-Lefftz, M., Altamimi, Z., 2011. Erratum to “On secular geocenter motion: The impact of climate changes” [Earth Planet. Sc. Lett. 296 (2010) 360–366]. *Earth Planet. Sc. Lett.* 306, 136. <https://doi.org/10.1016/j.epsl.2011.03.026>.

- Métivier, L., Greff-Leffitz, M., Diament, M., 2006. Mantle lateral variations and elastogravitational deformations—I. Numerical modelling. *Geophys. J. Int.* 167 (3), 1060–1076. <https://doi.org/10.1111/j.1365-246X.2006.03159.x>.
- Métivier, L., Rouby, H., Rebischung, P., Altamimi, Z., 2020. ITRF2014, Earth figure changes, and geocenter velocity: implications for GIA and recent ice melting. *J. Geophys. Res.* 125. <https://doi.org/10.1029/2019JB018333>, e2019JB018333.
- Mitrovica, J.X., Wahr, J., Matsuyama, I., Paulson, A., 2005. The rotational stability of an ice-age earth. *Geophys. J. Int.* 161 (2), 491–506. <https://doi.org/10.1111/j.1365-246X.2005.02609.x>.
- Moreaux, G., Lemoine, F.G., Capdeville, H., Kuzin, S., Otten, M., Štěpánek, P., Willis, P., Ferrage, P., 2016. The International DORIS Service contribution to the 2014 realization of the International Terrestrial Reference Frame. In: Lemoine, F., Schrama, E.J.O. (Eds.), *DORIS Special Issue: Scientific Applications of DORIS in Space Geodesy*. *Adv. Space Res.* 58(12), 2479–2504, doi: 10.1016/j.asr.2015.12.021.
- Morel, L., Willis, P., 2005. Terrestrial reference frame effects on global sea level rise determination from TOPEX/Poseidon altimetric data. *Adv. Space Res.* 36 (3), 358–368. <https://doi.org/10.1016/j.asr.2005.05.113>.
- Paulson, A., Zhong, S., Wahr, J., 2007. Limitations on the inversion for mantle viscosity from postglacial rebound. *Geophys. J. Int.* 168, 1195–1209. <https://doi.org/10.1111/j.1365-246X.2006.03222.x>.
- Pearlman, M.R., Degnan, J.J., Bosworth, J.M., 2002. The international laser ranging service. *Adv. Space Res.* 30 (2), 135–143. [https://doi.org/10.1016/S0273-1177\(02\)00277-6](https://doi.org/10.1016/S0273-1177(02)00277-6).
- Peltier, W.R., 1974. The impulse response of a Maxwell Earth. *Rev. Geophys.* 12 (4), 649–669. <https://doi.org/10.1029/RG012i004p00649>.
- Peltier, W.R., 1998. Postglacial variations in the level of the sea: Implications for climate dynamics and solid-Earth geophysics. *Rev. Geophys.* 36 (4), 603–689. <https://doi.org/10.1029/98RG02638>.
- Peltier, W.R., 2004. Global Glacial Isostasy and the Surface of the Ice-Age Earth: the ICE-5G (VM2) Model and GRACE. *Ann. Rev. Earth and Planet. Sci.* 32, 111–149. <https://doi.org/10.1146/annurev.earth.32.082503.144359>.
- Peltier, W.R., Argus, D.F., Drummond, R., 2015. Space geodesy constrains ice age terminal deglaciation: the global ICE-6G8C (VM5a) model. *J. Geophys. Res.* 119. <https://doi.org/10.1002/2014JB011176>.
- Rebischung, P., Altamimi, Z., Ray, J., Garayt, B., 2016. The IGS contribution to ITRF2014. *J. Geodesy* 90 (7), 611–630. <https://doi.org/10.1007/s00190-016-0897-6>.
- Riddell, A.R., King, M.A., Watson, C.S., Sun, Y., Riva, R.E.M., Rietbroek, R., 2017. Uncertainty in geocenter estimates in the context of ITRF2014. *J. Geophys. Res.: Solid Earth* 122. <https://doi.org/10.1002/2016JB013698>.
- Rignot, E., Velicogna, I., van den Broeke, M.R., Monaghan, A., Lenaerts, J., 2011. Acceleration of the contribution of the Greenland and Antarctic ice sheets to sea level rise. *Geophys. Res. Lett.* 38, L05503. <https://doi.org/10.1029/2011GL046583>.
- Schuh, H., Behrend, D., 2012. VLBI: A fascinating technique for geodesy and astrometry. *J. Geodyn.* 61, 68–80. <https://doi.org/10.1016/j.jog.2012.07.007>.
- Shepherd, A., Ivins, E.R., A, G., Barletta, V.R., Bentley, M.J., Bettadpur, S., Briggs, K.H., Bromwich, D.H., Forsberg, R., Galin, N., Horwath, M., Jacobs, S., Joughin, I., King, M.A., Lenaerts, J.T.M., Li, J., Ligtenberg, S.R.M., Luckman, A., Luthcke, S.B., McMillan, M., Meister, R., Milne, G., Mougouinot, J., Muir, A., Nicolas, J.P., Paden, J., Payne, A.J., Pritchard, H., Rignot, E., Rott, H., Sandberg Sorensen, L., Scambos, T.A., Scheuchl, B., Schrama, E.J.O., Smith, B., Sundal, A.V., van Angelen, J.H., van de Berg, W.J., van den Broeke, M., Vaughan, D.G., Velicogna, I., Wahr, J., Whitehouse, P.L., Wingham, D.J., Yi, D., Young, D., Zwally, H.J., 2012. A reconciled estimate of ice-sheet mass balance. *Science* 338, 1183–1189. <https://doi.org/10.1126/science.1228102>.
- Simms, A.R., Rouby, H., Lambeck, K., 2016. Marine terraces and rates of vertical tectonic motion: The importance of glacio-isostatic adjustment along the Pacific coast of central North America. *GAS Bull.* 128 (1–2), 81–93. <https://doi.org/10.1130/B31299.1>.
- Soudarin, L., Cazenave, A., 1995. Large-scale tectonic plate motions measured with the DORIS space geodesy system. *Geophys. Res. Lett.* 22 (4), 469–472. <https://doi.org/10.1029/94GL03382>.
- Tamisiea, M.E., Mitrovica, J.X., Davis, J.L., 2007. GRACE gravity data constrain ancient ice geometries and continental dynamics over Laurentia. *Science* 316, 881–883. <https://doi.org/10.1126/science.1137157>.
- Tregoning, P., Ramillien, G., McQueen, H., Zwart, D., 2009. Glacial isostatic adjustment and nonstationary signals observed by GRACE. *J. Geophys. Res.* 114, B06406. <https://doi.org/10.1029/2008JB006161>.
- van der Wal, W., Whitehouse, P.L., Schrama, E.J., 2015. Effect of GIA models with 3D composite mantle viscosity on GRACE mass balance estimates for Antarctica. *Earth Planet. Sci. Lett.* 414, 134–143. <https://doi.org/10.1016/j.epsl.2015.01.001>.
- Velicogna, I., Sutterley, T.C., van den Broeke, M.R., 2014. Regional acceleration in ice mass loss from Greenland and Antarctica using GRACE time-variable gravity data. *J. Geophys. Res. Space Phys.* 41, 8130–8137. <https://doi.org/10.1002/2014GL061052>.
- Willis, P., Bar-Sever, Y.E., Tavernier, G., 2005. DORIS as a potential part of a Global Geodetic Observing System. *J. Geodyn.* 40 (4–5), 494–501. <https://doi.org/10.1016/j.jog.2005.06.011>.
- Wu, P., Wang, H., Schotman, H., 2005. Postglacial induced surface motions, sea-levels and geoid rates on a spherical, self-gravitating laterally heterogeneous earth. *J. Geodyn.* 39 (2005), 127–142. <https://doi.org/10.1016/j.jog.2004.08.006>.
- Willis, P., Fagard, H., Ferrage, P., Lemoine, F.G., Noll, C.E., Noomen, R., Otten, M., Ries, J.C., Rothacher, M., Soudarin, L., Tavernier, G., Valette, J.-J., 2010. The International DORIS Service: toward maturity. *Adv. Space Res.* 45 (12), 1408–1420. <https://doi.org/10.1016/j.asr.2009.11.018>.
- Wu, X., Collilieux, X., Altamimi, Z., Vermeersen, B.L.A., Gross, R.S., Fukumori, I., 2011. Accuracy of the international terrestrial reference frame origin and earth expansion. *Geophys. Res. Lett.* 38, L13304. <https://doi.org/10.1029/2011GL047450>.